

Adsorption of Polymers at the Surface Concentrations in the Diluted to Semidiluted Regimes

Andrij Voronov, Igor Luzinov,[†] Serhiy Minko,^{*,‡} and Alexander Sidorenko

Lviv Department of Physical Chemistry Institute, Naukova str. 3a, 290053 Lviv, Ukraine

Eduard Vakarin and Myroslav Holovko

Institute for Condensed Matter Physics, Svientsitsky str. 1, 290011 Lviv, Ukraine

Received April 1, 1997; Revised Manuscript Received August 11, 1997[®]

ABSTRACT: The polymer adsorption regimes that correspond to very diluted bulk concentration and diluted to semidiluted surface concentration (on the solid substrate) were studied both theoretically and experimentally. The extremal behavior of the adsorbed polymer layer was observed experimentally with two independent methods: (1) contact angle measurements of adsorbed polymer films of poly(nonyl acrylate) and poly(methyl methacrylate) (PMMA) on the surface of aluminum foil and (2) electrochemical reduction of $K_3Fe(CN)_6$ on the surface of a platinum electrode covered by the adsorbed polymer layer. As recently reported (*Adsorp. Sci. Technol.* **1996**, 14, 251), the same behavior was observed on the surface of ZnO powder. The extremal behavior was found at polymer concentrations of about 0.001% in the bulk, or 1–5% from the plateau adsorption value. We suggest these data can be explained by the sharp change of conformation (and fraction of bonded units per chain) of adsorbed macromolecules when the transition from the diluted to semidiluted regime occurred. The calculations performed on the basis of the partition function combined with an associative integral equation predict the extremum in the surface coverage due to specific dependence of the intramolecular correlation function on the volume concentration of polymer.

Introduction

The experimental investigations and theoretical studies by mean field approximation and the scaling approach of polymer adsorption phenomena have been summarized in several reviews.^{1–4} The adsorption on an attractive surface from the diluted polymer solution causes the adsorption of isolated chains on the surface. This regime was not a subject of extensive experimental investigations. The poor development of this research was due to (1) the technical problems in studying the adsorbed layer with a very small amount of the polymer on the surface and (2) the fact that the most interesting, from a practical point of view (colloidal stabilization or flocculation), are saturated adsorbed layers a little below and about the plateau regime.⁵

The theoretical analysis performed by Bouchaud and Dauod⁶ predicted three regimes of polymer adsorption when the bulk concentration is increased: two-dimensional dilute, two-dimensional semidilute, and plateau regimes. In the first two cases, corresponding to very dilute bulk solution, the surface coverage is proportional to the bulk concentration according to the exponential Boltzmann prefactor with argument em ,^{3/5} where m is the number of units of the polymer and e is the attractive energy per monomer on the surface. In the plateau regime, the surface coverage increases logarithmically with bulk volume fraction ϕ_b . All these relationships result in a Langmuir-like adsorption isotherm, as has been shown in numerous experimental studies. The surface tension drops linearly with ϕ_b in the first and second regimes, and it is almost constant in the

plateau regime. The second regime is most interesting for investigations since there is a great difference between the bulk, which is dilute, and surface, which is semidilute. The transition from the dilute to semidilute regime on the surface, when the adsorbed macromolecules strongly interact with each other, occurs when the surface fraction of polymer (Γ) is larger than Γ_* , where $\Gamma_* \sim m^{-1/2}e^{-1/2}$. The longitudinal radius of a chain is expressed for dilute regime as $R_{||} \sim m^{3/4}e^{1/4}a$ and semidilute regime $R_{||} \sim m^{1/2}\Gamma^{-1/2}a$ (a is the step length). Therefore, the theory predicts the change of adsorbed chain conformation when the surface coverage is increased from the dilute to semidilute regime and the coverage amount is suggested to be a monotonous function of bulk concentration. However, the theory does not offer any prediction for the behavior of the adsorbed layer in the transition from the dilute to semidilute regime. To our knowledge, this transition region has not been identified experimentally so far.

In this paper we study the structure of an adsorption layer formed at a very dilute bulk concentration to find the region of the bulk and surface concentrations that should correspond to the transition from the two-dimensional dilute to two-dimensional semidilute regime. For this we used dewetted polymer adsorbed layers. It is very difficult to find an appropriate method to study the adsorbed layer exactly at equilibrium conditions with very small traces of the polymer on the surface. However, the prepared polymer covering after the solution was removed could be studied by means of application of the range of ordinary methods, e.g., kinetics measurement of heterogeneous chemical or electrochemical reactions and the contact angle method. It is necessary to distinguish the dewetted layer from the adsorbed polymer layer under equilibrium conditions in a solution–solid system. Of course, there is a relationship between the properties of the dewetted and the adsorbed polymer layer in equilibrium conditions. The relationship is governed first and foremost by the very close surface concentration of a polymer, because

* To whom correspondence should be sent.

[†] Current address: Center for Education and Research on Macromolecules, University of Liege, Sart-Tilman B6, 4000 Liege, Belgium.

[‡] Current address: Department of Experimental Physics, University of Ulm, Albert-Einstein-Allee 11, D-89069, Germany.

[®] Abstract published in *Advance ACS Abstracts*, October 1, 1997.

the amount of adsorbate left after the separation from solution and subsequent rinsing with solvent in many cases remains virtually unchanged, as compared to its equilibrium value,⁷ owing to the high affinity of macromolecules to the adsorbent surface.

Using the kinetic method, the relationship with extremum between the fraction of surface capped by polymer and bulk polymer concentration for very dilute φ_b values was observed.⁸ We presumed that this behavior of the beforehand polymer film is caused by the nonmonotonous change of the adsorbed layer during the transition from single adsorbed chains regime (two-dimensional dilute) to the two-dimensional semidilute regime. In this paper we present the corroboration of the above mentioned effect due to experiments with two different techniques: contact angle and electrochemical reaction measurements.

In order to provide qualitative insights on the phenomena occurring at the transition from dilute to semidilute regimes, we consider two simple models for adsorption of polymers at attractive surfaces. The primary purpose of our theoretical approach is to analyze several factors that may have a significant effect on the interfacial behavior. In particular, we investigate the role of localization and activity of adsorbing sites at the surface in determining the surface coverage θ and its dependence on the polymer length m and flexibility L . The polymer is modeled by a chain of fused hard sphere segments. The segments are allowed to penetrate each other and, consequently, the distance between two adjacent beads can be smaller than the diameter of the segments. Similar models for polymeric liquids have been developed on the basis of the polymer reference interaction site model of Schweizer and Curro⁹ and the density functional theory of Kierlik and Rosinberg.¹⁰ Yethiraj and Hall¹¹ have performed numerous computer simulations both in the bulk and at the interface. On the basis of Wertheim's theory¹² for associating liquids, Chang and Sandler¹³ have proposed the so-called ideal chain approximation within the multidensity integral equation theory. In our previous studies,^{14,15} we have suggested that the change of overlapping L between the segments corresponds to restriction imposed on the polymer flexibility. Thus the case of $L = 1$ describes the totally flexible chains, while $1/2 < L < 1$ corresponds to semiflexible polymers. This factor has a significant effect on the intramolecular correlations,¹⁴ which are closely related to conformation characteristics (radius of gyration,¹⁶ etc.). The surface is modeled as a sticky hard wall¹⁷ (homogeneous model) and later as a wall with a lattice of sticky sites¹⁸ (periodical model). These models represent only two essential features of the surface side: spatial restriction and adsorptive activity. However, we expect them to be sufficient for qualitative exploration of the interfacial effects induced by the polymer subsystem.

We calculate the fraction θ of the surface covered through the associative Henderson–Abraham–Barker equation^{19,20} and also by means of the partition function calculation.²⁰ In both approaches the low-density (concentration) extremum in θ is observed. We show that the peculiarity in the surface coverage is induced by the intramolecular correlations along the chains. Since the intramolecular correlations are responsible for the conformational changes at low densities, we conclude that the extremum in θ is due to conformational variations at the interface, induced by varying polymer concentration.

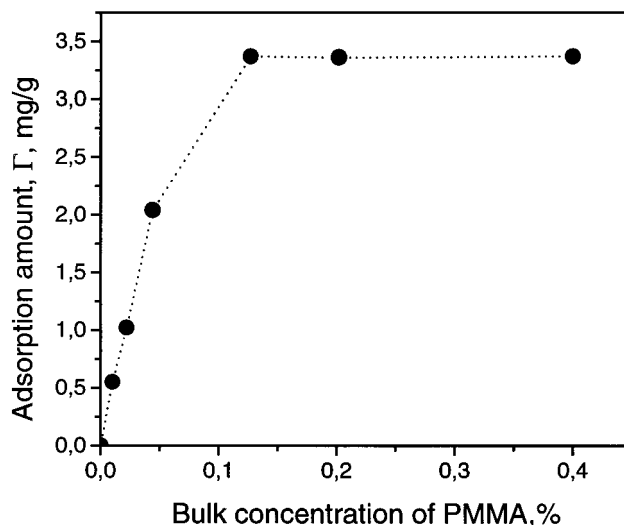


Figure 1. Adsorption isotherm of PMMA on aluminum powder from ethyl acetate.

Experimental Section

Polymer Synthesis. Poly(nonyl acrylate) (PNA) for contact angle experiments ($M_n = 10^5$) was synthesized by free radical polymerization in butyl acetate with benzoyl peroxide as a radical initiator at 60 °C. Poly(methyl methacrylate) (PMMA) for electrochemical and contact angle experiments ($M_n = 7.9 \times 10^4$) was synthesized by free radical polymerization in butyl acetate with AIBN as a radical initiator at 70 °C. The monomers were distilled and kept under argon. The polymerization was stopped at 30% conversion. After synthesis, the polymer was purified by multiple reprecipitation.

Polymer Solution Preparation. After the synthesis, the purified polymers were used to prepare 0.6% butyl acetate or ethyl acetate solutions. The solvents were of analytical grade and were used as received. To remove from the solutions a fraction of the polymer having a higher adsorption activity (high molecular weight fraction or/and fraction with some amount of the acid units in the chain of the polymer or other possible contamination), 10 g of Al_2O_3 (specific surface, 1 m²/g) was added to each 100 mL of the solution. The suspensions were stirred for 24 h. After stirring the adsorbent was removed by centrifugation (8000 min⁻¹). The obtained solution was analyzed for the evaluation of the polymer concentration and used in the following experiments and for preparing of the solutions of various concentrations.

Sample Preparation. Plates of aluminum foil were subsequently rinsed with distilled water, acetone, and again with water, and then these plates were heated in a muffle oven at 450 °C for 4.5 h.

To prepare the plates with a saturated adsorbed layer of the polymer, they were immersed in the 0.5% solution (see below) of the polymer at room temperature for 24 h. Then the plates were taken out of the solutions and rinsed six times in butyl acetate and dried at room temperature.

To determine the polymer content on the surface of the adsorbent, the following procedure was employed. A weighed portion of Al_2O_3 was added to a 0.5% solution of the polymer (i.e., the solution corresponding to the plateau regime) and the mixture stirred. After 24 h the adsorbent was separated by the centrifugation, rinsed six times in the solvent, and dried at room temperature and under vacuum at 100 °C. The content of the adsorbate was evaluated by the weight loss of the powder sample after burning in the muffle oven at 500 °C for 5 h.

It has been shown experimentally, by measuring the adsorption isotherm (e.g., for PMMA, see Figure 1), that for the employed adsorbate solution–adsorbent ratio (5:1) the 0.5% PMMA solution corresponds to a plateau region at the isotherm.

For preparation of the specimens with an amount of the adsorbed polymer smaller than that in the saturated adsorp-

tion layer, the following procedure was used. As the first step, from the 0.5% solutions of the polymers, the range of diluted solutions was prepared by adding the solvent. In the second step, 5 g of Al_2O_3 was added to each 25 mL of diluted solution and the mixture stirred. After sedimentation of Al_2O_3 (2 days), the plates of aluminum foil were carefully immersed into the solutions for 72 h. (It has been shown experimentally that after this time the contact angle of water on the plate surface was not changed.) Then the plates were taken out of the solutions and rinsed six times in butyl acetate and dried at room temperature. The main purpose of this procedure is to use the aluminum powder to control the equilibrium polymer concentration in a region of very small concentrations and prepare the plates with a small amount of adsorbed polymer.

The adsorbent was used to determine the polymer adsorption amount. It is possible, by using the gravimetric technique, to measure the adsorbed amount only for relatively high values of the adsorption (more than 10% of the plateau adsorption amount). Therefore, for the large adsorption values we used measured magnitudes. For the diluted regime, we calculated Γ magnitudes from the dilution index by taking into account that for this regime Γ is proportional to the bulk concentration: $\Gamma = \Gamma_{10}c/c_{10}$, where Γ_{10} and c_{10} are the adsorption amount and equilibrium bulk concentration of polymer, where $\Gamma_{10} = 0.1\Gamma_{\text{plateau}}$, and c is the equilibrium bulk concentration, which corresponds to the Γ magnitude.

"Unbonded" thick polymer films (the thickness of these films makes it possible to ignore the effect of a substrate surface) were prepared from 10% polymer solutions on the glass plates. The solution was poured on the plate and left for evaporation of the solvent.

Contact Angle Measurements. The static contact angles of water were determined using the sessile drop method. A drop (0.001 mL) of double distilled water was put on the plate surface with a microliter syringe. The diameter (d) and height (h) of the drop were measured by cathetometer. The contact angle value was computed as $\tan(\theta/2) = 2h/d$. Measurements were run every 2 min after the drop was rested on a surface. For each sample, three measurements on three plates were made. In most cases, the root-mean-square deviation did not exceed $1-2^\circ$.

Electrochemical Reaction on the Pt Electrode. The rotated disk electrode (RDE) was made of Pt wire with diameter 1 mm in a Teflon sheath. The rotating speed was 300 rpm. The potential of the RDE was measured against a reference saturated AgCl electrode. Pt foil (0.7 cm^2) was used as a counter electrode. The RDE before each experiment was cleaned by emery cloth, damp paper filter, and ultrafine Cr_2O_3 powder and then with damp and dry paper filter. The electrochemical cell was supplied with a Luggin capillary and filled with the solution of $5 \times 10^{-3} \text{ mol/L K}_3\text{Fe}(\text{CN})_6$ and 0.1 mol/L KCl. Ar was bubbled through the solution during experiments. The reproducibility of the measurement was achieved by keeping the electrode in the solution at potential $E = 0.0 \text{ V}$ for 150 s, then 1 s at -0.50 V , and then at change from 0.50 to 0.00 V with scan rate $5 \times 10^{-2} \text{ V/s}$. The RDE was then rinsed with distilled water, acetone, and ethyl acetate and dried for 3 min. Following that, the RDE was immersed into the solution of PMMA under precipitated aluminum powder (see the Sample Preparation section) and kept in the solution for 5 h. Finally, it was rinsed by ethyl acetate and distilled water and immersed again into the cell to obtain the volt-ampere curve. The volt-ampere curves were used to obtain parameters of $\text{Fe}(\text{III})$ reduction on the RDE surface according to the following equation:²¹ $I = qFCS/(n^{-1} + k^{-1})$, where I is the current intensity, q is the ion charge, F is the Faraday constant, C is the $\text{K}_3\text{Fe}(\text{CN})_6$ concentration, S is the electrode surface, n is the mass transfer rate, $k = k_h \exp(-\alpha F/(RT(E - E_{1/2})))$, k_h is the charge transfer rate constant, α is the dimensionless transfer coefficient, and E and $E_{1/2}$ are the potential and half-wave potential, respectively. Experimental data were processed using Markvard method to evaluate k_h , n , and α .

Theory

Model of the Polymer. We model the polymer molecule as a chain consisting of fused, hard spherical segments. The mean chain length (the degree of polymerization) is denoted as m . The dimensionless volume concentration of polymer segments is $c = \rho d^3$, where ρ is the number density of segments and d is the hard core diameter of a given segment. Since the segments are fused, they are allowed to penetrate each other, and thus, the distance between two adjacent beads is L , with $L/d \leq 1$. As suggested in our previous studies,^{14,15} by changing the bond length L , we can change the macromolecule flexibility. In particular, the angle ω between two adjacent beads is restricted to

$$2 \arcsin\{1/2L\} \leq \omega \leq \pi \quad (1)$$

Thus, $L = 1$ corresponds to totally flexible chains. The flexibility decreases with decreasing L up to $L = 1/2$. Note that the above model ignores influence of the solvent on the behavior of the polymer subsystem. In fact, the solvent can be thought of in this case as a fictitious medium that separates the polymers in such a way that the volume concentration of the polymer is $K = c/m$. This simplification seems to be reasonable, since the role of the solvent is expected to be of secondary importance in determining the adlayer properties at low polymer concentration, especially for a Θ -solvent and when the polymer-surface attraction is stronger than the solvent-surface attraction. Consequently, the value $\eta = \pi d/6$ will be chosen as a dimensionless measure of bulk concentration of polymer segments.

Model of the Surface. In order to investigate the role of localization of adsorbing sites, we consider two models of the surface. The first (*homogeneous adsorption model*) describes the surface as a hard plane wall with a uniform adhesive layer. This is the case of the so-called "mobile" adsorption in which the adsorbate can freely move along the wall. The wall-segment potential $U(x)$ is

$$U(x) = U_{\text{hw}}(x) + U_{\text{st}}(x) \quad (2)$$

where $U_{\text{hw}}(x)$ is the hard wall potential and $U_{\text{st}}(x)$ is the sticky potential defined as

$$\exp\{-\beta U_{\text{st}}(x)\} = 1 + \lambda \delta(x - d/2) \quad (3)$$

This relation states that a polymer segment should touch the surface in order to be adsorbed. Here x is the distance to the wall, λ is the stickiness parameter, and β is the Boltzmann thermal factor. Note that we do not consider the terminal segments; that is, all the segments of a chain have the same affinity to the surface.

In the second model (*periodical adsorption model*) the surface is described as the hard wall with a regular array of point adsorbing sites. In this case the adsorbing potential is a function of position \mathbf{r}

$$\exp\{-\beta U_{\text{st}}(\mathbf{r})\} = 1 + \lambda \delta(x - d/2) \sum \delta(R - R_i) \quad (4)$$

where the summation is over the lattice positions R_i . In this case we deal with strongly localized adsorption, which is relevant to crystalline solid adsorbents. Note that the aluminum foil used in the experiment has a random distribution of adsorbing sites, i.e., it is neither uniform nor crystalline. Therefore, we consider two

extremal distributions of adsorbing sites. The real distribution is expected to lie between those two measures.

Integral Equation Approach. For the homogeneous adsorption model the wall-segment correlation functions $h_{iw}(x)$ are determined by the associative Henderson-Abraham-Barker integral equation:

$$h_{iw}(x) = c_{iw}(x) + \sum_{lm} \int dr C_{il}(r) \sigma_{lm} h_{mw}(x-r) \quad (5)$$

Here $c_{iw}(x)$ are the direct wall-segment correlation functions and $C_{il}(r)$ are the bulk segment-segment direct correlation functions. Each of the indices i, l, m is assigned the values of 0, 1, 2, which correspond to different types of segments. In particular, the function $C_{12}(r)$ describes both the intra- and intermolecular direct correlation between single and double bonded segments, a distance r apart. The index w corresponds to the wall and the index 0 accounts for the hard core contributions irrelevant to the bonding of the segments. Density parameters σ_{lm} are the elements of the matrix:

$$\sigma = \rho \begin{bmatrix} 1 & m^{-1} & m^{-1} & m^{-2} \\ m^{-1} & 0 & m^{-2} & 0 \\ m^{-1} & m^{-2} & 0 & 0 \\ m^{-2} & 0 & 0 & 0 \end{bmatrix} \quad (6)$$

It is worth noting that the above matrix as well as the bulk functions $C_{il}(r)$ are determined within the ideal chain approximation. The diagrammatic meaning of this approximation is discussed by Chang and Sandler¹³ and also in the previous studies^{14,15}. Note, however, that in this case the intramolecular correlations are described to be independent of excluded volume effects. The quantitative validity of this approximation is restricted to relatively high polymer concentrations, but for the purpose of qualitative analysis we will use it at low concentrations also.

In order to calculate the wall-segment correlation functions from eq 5, the latter should be supplemented by a closure condition. For this we propose the Percus-Yevick (PY) condition:

$$c_{iw}(x) = f_{hw}(x) y_{iw}(x) + \exp\{-\beta U_{hw}(x)\} f_{st}(x) y_{iw}(x) \quad (7)$$

where the cavity correlation function $y_{iw}(x)$ is related to the wall-segment correlation function by

$$1 + h_{iw}(x) = \exp\{-\beta[U_{hw}(x) + U_{st}(x)]\} y_{iw}(x) \quad (8)$$

Here $f_{hw}(x)$ and $f_{st}(x)$ are the Mayer functions for the hard wall and sticky potentials, respectively. After the partial correlation functions are calculated from eqs 5-8, the total correlation function $h(x)$ is defined by²⁰

$$h(x) = h_{0w}(x) + \frac{2}{n} h_{1w}(x) + \frac{1}{n} h_{2w}(x) \quad (9)$$

Then the segment density profile $\rho(x)$ consists of regular and singular (i.e., containing the δ -function) parts:¹⁸

$$\rho(x) = \rho[1 + h(x)] = \rho^{\text{reg}}(x) + \lambda \delta(x - d/2) \rho^{\text{sin } g}(x) \quad (10)$$

Integrating the singular part, we get the surface density ν of the adsorbed layer. After that we divide ν by the maximal possible coverage of the unit area at the surface and obtain the fraction θ of the covered surface:

$$\theta = \frac{\lambda \rho^{\text{sin } g}(d/2) A(n, \rho)}{1 + \lambda \rho^{\text{sin } g}(d/2) B(n, \rho)} \quad (11)$$

Where $A(n, \rho)$ and $B(n, \rho)$ are the functionals of the pair segment-segment correlation function $g_2(d)$ taken at contact position. In fact, $g_2(d)$ is connected with the lateral interaction in the adlayer, such that the values $A(n, \rho)$ and $B(n, \rho)$ tend to 1 when $g_2(d) \rightarrow 1$. Then eq 11 describes the coverage by independent segments. At a region of low polymer concentration the intramolecular part of the pair correlation is dominant:

$$g_2(d) \approx g_{\text{int}}(d) \propto \left(\frac{n-1}{n}\right)^2 \frac{1}{24\eta L^3} \quad (12)$$

At the same time, the intramolecular correlation function (for low η) coincides with the so-called connectivity correlation function.¹⁶ The latter gives a probability of finding two segments in the same chain, at a given distance apart. Integrating this function over the volume, one can find the radius of gyration, which is a measure of conformation. Thus, the peculiarities of θ at low polymer concentrations are due to the stickiness λ and the intramolecular correlation (polymer conformation) along a given chain. Note, however, that eq 12 is derived within the ideal chain approximation, which is only qualitatively correct at low η . On the other hand, Ghonasgi and Chapman have shown²² that the intramolecular correlations are dominant at low densities. This conclusion somewhat justifies our approximate estimation given by eq 12. Note in addition that we are restricted to λ low enough to keep the contact value $\rho^{\text{sin } g}(d/2)$ positive.¹⁷ This restriction results from the PY approximation used in our calculations.

Partition Function Approach. For the model of periodical adsorption the partition function Ξ can be rearranged to the two-dimensional Ising form¹⁸

$$\Xi = \sum_{\{t\}} \exp[-\beta w \sum_{ij} t_i t_j] \exp[-\beta \mu \sum_i t_i] \quad (13)$$

under the constraint that the segment diameter d approximates the mean spacing between the adsorbing sites at the wall. Here the occupation number t_i is 1 if the lattice site i is occupied by the segment and 0 if it is vacant. The value of W is the potential of the lateral interaction between adsorbed segments; the μ is connected with the external field at the i th adsorbing site. As we have shown earlier,²⁰ these values can be approximated by the contact values of the segment-segment pair correlation function and of the wall-segment correlation function, respectively. The mean force potential $W = -(1/\beta) \ln g_2(d)$ is again a crucial ingredient that determines the interfacial properties. Thus, the lateral interaction is attractive when $g_2(d) > 1$, $W < 0$. This may cause a two-dimensional condensation in the adlayer.^{18,20} As follows from eq 12, $g_2(d) \gg 1$ when η is low and also when $L < 1$. This indicates the influence of increasing concentration and decreasing flexibility on the lateral interaction.

The fraction of occupied sites θ (or the fraction of covered surface) can be determined by the differentiation of $\ln \Xi$ with respect to $\ln \lambda$. In the mean-field approximation, this procedure leads to a transcendental equation with respect to θ , which we have solved numerically to obtain θ for a triangular array of sticky sites. It is worth noting that, in contrast to the case of monoatomic fluids, the θ is not the adsorption isotherm

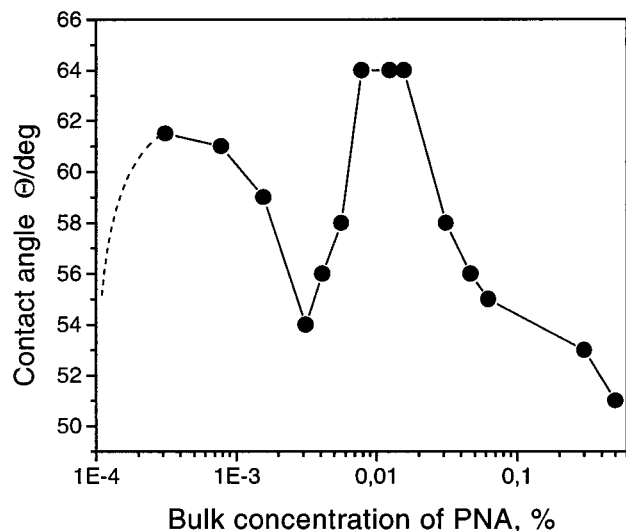


Figure 2. Plot of contact angle vs equilibrium bulk concentration of PNA in butyl acetate.

because a single polymer chain may occupy several adsorbing sites at the wall. In order to calculate the adsorption isotherm for our case, it is necessary to know a distribution of adsorbed segments per chain.

Results and Discussion

Contact Angle Measurements. The plot of the contact angle for wetting of the dewetted polymer covering obtained by adsorption of PNA vs bulk concentration of PNA in adsorption experiment is shown in Figure 2. The contact angles for the covered surface is smaller than that for the "unbonded" polymer film ($\Theta_p = 99^\circ$) but larger than that for the uncovered substrate ($\Theta_s = 38^\circ$). The reasons for this behavior were discussed recently.²³ It was found out that only part of a substrate is screened by the adsorbed polymer film, leaving wetting liquid in contact with both the polymer and the surface of a substrate. In order to apply quantitative parameters, a model based on the Cassie equation²⁴ was proposed. According to the model, the surface of a substrate covered by an adsorbed polymer film is considered as a planar heterogeneous surface with two types of sites: sites where the wetting liquid is in contact with polymer alone, and sites where the liquid is in contact only with the substrate surface:

$$\cos(\Theta_a) = \theta \cos(\Theta_p) + \epsilon \cos(\Theta_s)$$

$$\theta + \epsilon = 1 \quad (14)$$

where θ is the fraction of the sites screened by polymer, ϵ is the part of substrate available for the wetting liquid, and Θ_a , Θ_s , and Θ_p are the contact angles for plates covered by adsorbed polymer film and uncovered plates with "pure" surface and thick polymer films, respectively. This equation is valid if the same fraction of polar segments is exposed on the surface of an adsorbed polymer chain and thick polymer film. The data (Figure 2) were replotted using eq 14 as θ vs $\Gamma/\Gamma_{\text{plateau}}$ ratio (Figure 3).

In both plots the extremum that corresponds to very small bulk PNA concentration ($\approx 0.0005\%$) is pronounced very well. This extremum, we suggest, should be ascribed to the change of θ forced by the change in conformation of adsorbed chains in the region of the transition from the two-dimension diluted to two-dimension semidiluted regime.

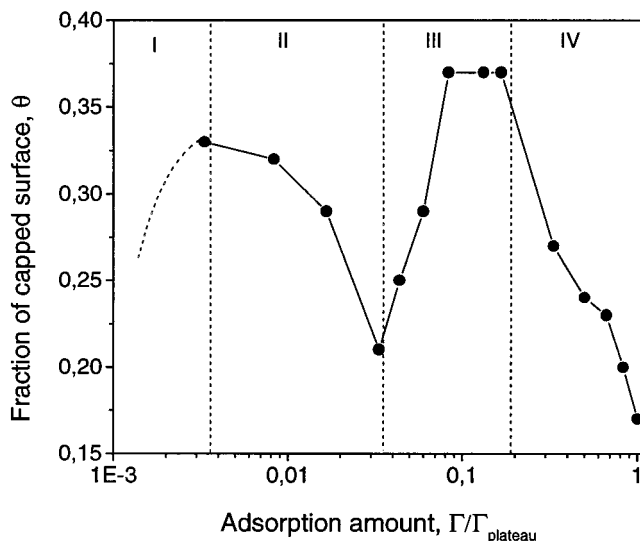


Figure 3. Plot of θ vs $\Gamma/\Gamma_{\text{plateau}}$ for an adsorption layer of PNA.

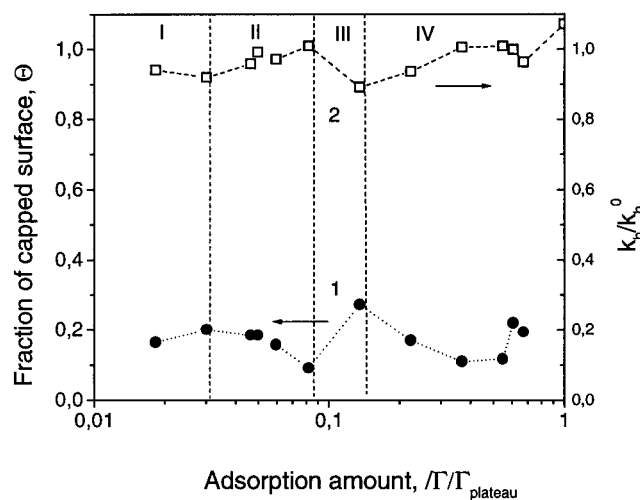


Figure 4. Plot of θ vs $\Gamma/\Gamma_{\text{plateau}}$ (1) and k_h/k_h^0 ratio vs $\Gamma/\Gamma_{\text{plateau}}$ (2) for an adsorption layer of PMMA.

Electrochemical Method. It is known that adsorption of molecules on the electrode surface changes properties of the double electric layer and diffusion of the reagents near the electrode surface. In this case, the charge transfer rate constant k_h can depend on the structure of the adsorbed polymer layer. Because in each electrochemical experiment the surface of RDE changes after each cleaning, we use, as a characteristic of the electrochemical reaction of Fe(III) reduction, the ratio k_h/k_h^0 , where k_h^0 is the charge transfer rate constant on the surface of uncovered RDE. The plot of k_h/k_h^0 ratio vs $\Gamma/\Gamma_{\text{plateau}}$ is shown in Figure 4.

The θ - $\Gamma/\Gamma_{\text{plateau}}$ relationship for the PMMA adsorption on the plate is presented in the same picture. One can see the reverse relationship of θ from $\Gamma/\Gamma_{\text{plateau}}$. This is in contrast to the k_h/k_h^0 ratio vs $\Gamma/\Gamma_{\text{plateau}}$ relationship for the low coverage of the surface. This indicates that the larger is the caption of the electrode surface the lower is the charge transfer rate constant. In this paper we do not discuss a mechanism of the process. The important conclusion is that the electrochemical measurements prove the sharp change in the adsorption layer in the same concentration region as in the case of contact angle measurements ($\Gamma/\Gamma_{\text{plateau}} \approx 0.03$).

Therefore, the contact angle isotherm could be separated into four sections (Figures 3 and 4, also compare Figures 1 and 4). The first corresponds to the increase

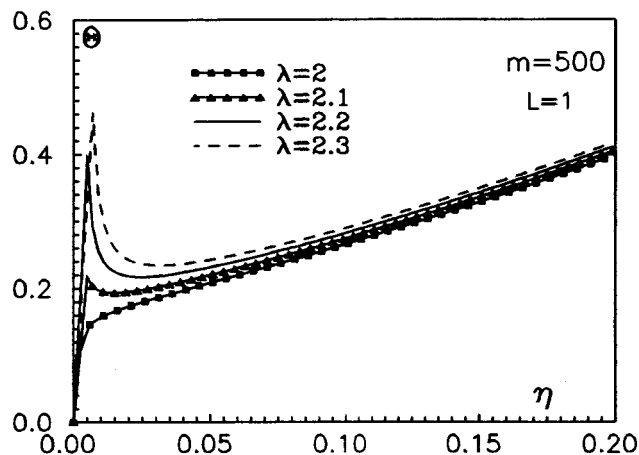


Figure 5. Plot of θ vs η at different λ . $L = 1$, $m = 500$.

in contact angle (i.e., decrease of the surface tension), as compared to the uncovered surface ($\Theta_s = 38^\circ$), due to the covering of the substrate by polymer proportionally to the concentration in the bulk. In the second region, we observe a sharp decrease in the contact angle, which we consider to be an extremal behavior. The third region corresponds to the further increase in the surface coverage and ends near the plateau region. The last region (IV) corresponds to the saturated adsorption layer where the further increase in adsorption is accompanied by the decrease in the fraction of bonded segments per chain. The latter results in the increase in the permeability of the adsorbed layer. We may presume that wetting liquid (water) can rearrange the adsorbed layer of weakly adhered chains. Nevertheless, for the PMMA layer one can see the subsequent increase in the contact angle (or the fraction of capped surface). That means that density and permeability of the saturated adsorbed layer depends on the size of the alkyl substituent in the acrylate monomers.²⁵ Molecular weight polydispersity is another possible explanation of such behavior in the saturated layer. In this paper we do not consider the concentrated adsorbed polymer layers.

At the diluted regime, which corresponds to section I, the growth of θ is caused by the increase of a number of adsorbed chains. Section II corresponds to the semidiluted concentration regime, when the chain reformation causes the sharp decrease in θ . The following growth of the adsorbed polymer amount (sections III and IV) is accompanied by a chain reformation. Such reformation was well documented experimentally in kinetic adsorption measurements and numeric models by Pefferkorn *et al.*²⁶ At regimes of sections III and IV the change of θ values is caused by at least two factors: the growth of the number of adsorbed chains and the change of the fraction of attached segments per chain.

Homogeneous Adsorption Model. Theoretical results for the fraction of covered surface θ as a function of dimensionless bulk segment concentration (or the packing fraction) $\eta = c\pi/6$ are displayed in Figures 5–7. The θ curve has a sharp extremum at low concentrations. Note that such a simple model allows one to predict several regions detected experimentally. First is the so-called dilute regime in which the coverage grows linearly with η . As mentioned above, this regime is connected with adsorption of distinct chains that are almost independent of each other. As suggested by Ghonasgi and Chapman²¹ and also in our previous

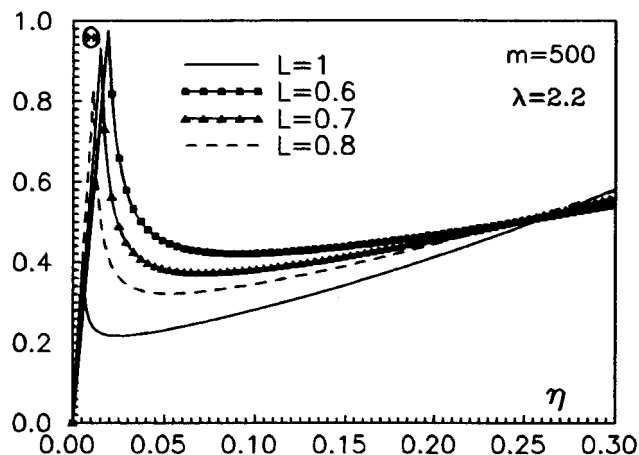


Figure 6. Plot of θ vs η at different L . $\lambda = 2.2$, $m = 500$.

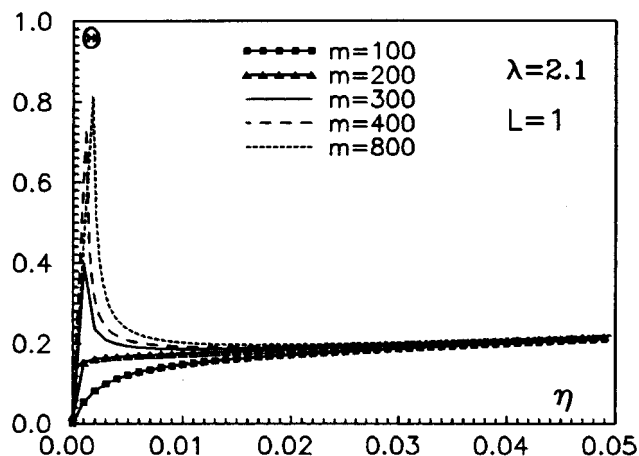


Figure 7. Plot of θ vs η at different m . $\lambda = 2.1$, $L = 1$.

papers,^{14,20} the intramolecular correlations in a chain play a dominant role in this case because η is very low. As the coverage and the chain concentration increase to certain extremal values θ^* and η^* , one can see the transition to the semidilute regime in which there is a competition between the intra- and intermolecular correlations. At this stage, the coverage decreases due to the weakening of the intramolecular correlations, which are known to be closely related to the conformation properties of polymer chains. This allows us to treat the decrease in θ as a change of polymer conformation in the adlayer due to increasing polymer concentration. In particular, this change may be related to the interfacial chain–blob transition, which leads to an increase of free surface. After that, the so-called concentrated regime occurs, in which the coverage grows slowly with concentration, up to the saturation (plateau) point.

In Figure 5 the plot of θ vs η at different λ is depicted. The plot indicates that the increase in stickiness allows us to achieve a higher coverage. One can observe a competition between the wall–segment attraction and the conformational variations induced by increasing polymer concentration. The wall tends to hold a conformation suitable for the planar geometry, while the intramolecular correlations along the polymers together with packing effects lead to the swelling of the chains, the phenomenon typical for dense polymer melts.^{4,7} Therefore, at low λ ($\lambda = 2$), the adsorbing potential is too weak to hold the planar shape of the adsorbate, and θ is a monotonous function of η . This condition persists up to some extremal value of $\lambda = \lambda^*$. When $\lambda > \lambda^*$, we

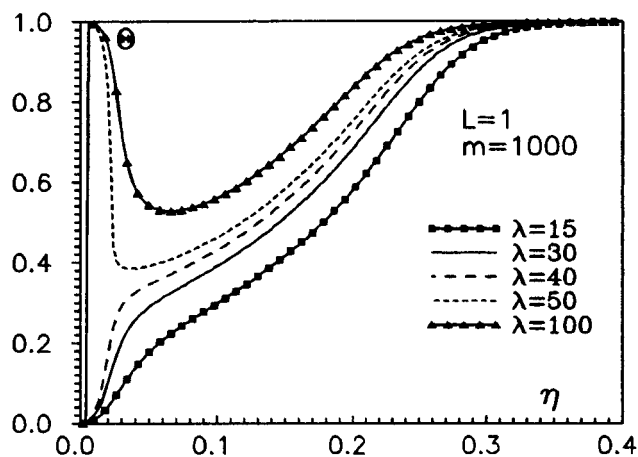


Figure 8. Plot of θ vs η for the localized adsorption model.

have a sharp increase in the coverage until the extremal concentration $\eta = \eta^*$ is reached. As indicated by Figure 5, η^* increases with increasing stickiness. The coverage decreases when $\eta > \eta^*$ because the changes induced by increasing concentration become dominant. With the further increase in η , θ increases slowly. At this stage the packing is a leading process and the surface has only minor influence. In this way we approach the saturation (plateau) at $\eta = \eta_p$. We have analyzed the ratio $R = \eta^*/\eta_p$, which indicates the difference between extremal and plateau concentrations. Because both Γ and η are proportional to the polymer weight concentration, this value corresponds to the experimentally measured $\Gamma/\Gamma_{\text{plateau}}$ ratio. The results for R obtained within our theoretical approach are in agreement with experimental data ($0.01 < R < 0.05$).

Figure 6 displays the effect of overlapping on the extremal behavior of θ : η^* increases with decreasing L (or with decreasing flexibility). This conclusion is physically reasonable since more rigid chains are expected to change their conformation at higher concentrations. An interesting feature is the crossing of curves drawn for different L at $\eta \approx 0.27$. This point may serve as a border of semidiluted and concentrated regimes. At concentrations higher than the cross-point, the curves exhibit a "reverse" order in comparison to that at $\eta < 0.27$. In particular, the curve for $L = 1$ (totally flexible chains) corresponds to highest θ . This behavior results from an interplay between chain flexibility and their packing properties. In fact, more flexible chains are expected to form a close packed adlayer easier than semi-flexible polymers. The ratio R is again in a good agreement with experiment in a wide range of L .

Dependence of the extremal behavior on the polymer length is shown in Figure 7: θ increases with increasing m at $\eta < \eta^*$ (i.e., when the chains are almost independent from one other). After that, θ decreases for the reason discussed above. The extremal value η^* increases with increasing m , because longer chains have more adsorbed segments. Therefore, higher concentrations are required to change their conformation. This is in contrast to the bulk behavior, where long chains possess substantial conformational entropy, and therefore, change their conformation easier.

Periodical Adsorption Model. The fraction of the surface covered is plotted for this case in Figure 8. All the principal features detected within the homogeneous model take place also in this case. In particular, θ increases with increasing concentration as well as with increasing λ . One can observe a hump appearing as a

result of the competition between the inter- and intramolecular correlations at low η . The hump grows with increasing λ . The main feature, due to the regular lattice, is the possibility for a cooperativity in the adlayer.¹⁸ In this case, we have a two-dimensional condensation of polymer segments at low concentrations when λ is high enough to support this process. This effect is manifested by a sharp increase in the coverage due to the adsorption of distinct chains. As the concentration increases, the intermolecular correlation becomes important. This results in the decrease in θ due to the conformational variations. A detailed analysis of this cooperative phenomenon is reported in the previous paper.²⁰ The ratio R for this case is higher than for a uniform surface model but still remains within the 1–5% observed experimentally. Note that we have displayed the case for $L = 1$ only, because the modifications caused by varying flexibility are similar to those detected for the uniform surface.

Conclusions

The probing of the solid substrate covered by the adsorbed polymer layer with contact angle and electrochemical methods permitted us to identify the extremal behavior in the fraction of capped surface vs adsorbed amount. Combined with previously reported data,²³ the experimental facts indicate the existence of a sharp change in the polymer adlayer structure formed in very diluted polymer solutions. We assume that this extremal behavior corresponds to the transition from the diluted to semidiluted two-dimensional regime of polymer chains at the solid surface.

The extremal behavior was also predicted by theoretical analysis performed using two simple models for adsorption of polymer chains at solid surfaces. It is shown that the extremum in the surface coverage occurs for both homogeneous and periodical adsorption models. The changes of this peculiarity with varying adsorption activity λ , polymer length m , and flexibility L are investigated. The origin of the extremum is the weakening of the intrachain correlation with increasing bulk concentration of polymer. Because the intramolecular correlation is the only reason for conformational changes at low concentrations, we can explain the extremal behavior of the surface coverage as a result of the conformational variations in the adlayer. We show that when the adsorbing sites form a regular lattice at the wall, the extremal behavior of θ may be of cooperative character. The relation between the extremal and plateau concentrations is in reasonably good agreement with experimental data. Because the plateau coverage in our models may achieve the values about 0.7–0.97, instead of $\theta \approx 0.4$ detected experimentally, we conclude that the model should be modified to account for the shielding effect of the adsorbing sites caused by the occupation of the neighbouring sites.

Acknowledgment. Financial support was provided by grant No. 4.4/60 and No. 2.4/174 of the Ukrainian Ministry of Science and Technology. S.M. thanks the Alexander von Humboldt Foundation for the support of this study.

References and Notes

- (1) Kawaguchi, M.; Takahashi, A. *Adv. Colloid Interface Sci.* **1992**, *37*, 219.
- (2) Takahashi, A.; Kawaguchi, M. *Adv. Colloid Interface Sci.* **1982**, *22*, 1.

- (3) Cohen-Stuart, M. A.; Cosgrove, V.; Vincent, B. *Adv. Colloid Interface Sci.* **1986**, *24*, 13.
- (4) de Gennes, P. G. *Adv. Colloid Interface Sci.* **1987**, *27*, 189.
- (5) Napper, D. H. *Polymer stabilisation of Colloidal Dispersions*; Academic Press: New York, 1983.
- (6) Bouchaud, E.; Daoud, M. *J. Phys.* **1987**, *48*, 1991.
- (7) Fleer, G. J.; Lyklema, J. In *Adsorption from Solution at the Solid/Liquid Interface*; Parfitt, G. D., Rochester, C. H., Eds.; Academic: London, 1983.
- (8) Minko, S.; Luzinov, I.; Evchuk, I. *Adsorp. Sci. Technol.* **1996**, *14*, 251.
- (9) Schweizer, K. S.; Curro, J. G. *J. Chem. Phys.* **1988**, *89*, 3342, 3350. Curro, J. G. *Macromolecules* **1994**, *27*, 4465.
- (10) Kierlik, E.; Rosinberg, M. L. *J. Chem. Phys.* **1994**, *100*, 1716. Phan, S.; Kierlik, E.; Rosinberg, M. L.; Yethiraj, A.; Dickman, R. *J. Chem. Phys.* **1995**, *102*, 2141.
- (11) Yethiraj, A.; Hall, C. K. *Macromolecules* **1991**, *24*, 709. Yethiraj, A.; Hall, C. K. *Mol. Phys.* **1991**, *73*, 503. Yethiraj, A.; Hall, C. K. *J. Chem. Phys.* **1989**, *91*, 4827.
- (12) Wertheim, M. S. *J. Stat. Phys.* **1984**, *35*, 19, 35. Wertheim, M. S. *J. Stat. Phys.* **1984**, *42*, 459, 477. Wertheim, M. S. *J. Chem. Phys.* **1987**, *87*, 7323.
- (13) Chang, J.; Sandler, S. I. *J. Chem. Phys.* **1995**, *102*, 437. Chang, J.; Sandler, S. I. *J. Chem. Phys.* **1995**, *103*, 3196.
- (14) Duda, Yu.; Vakarin, E.; Kalyuzhnyi, Yu. V.; Holovko, M. F. *Physica A*, in press.
- (15) Vakarin, E.; Duda, Yu.; Holovko, M. F. *J. Mol. Liq.*, in press.
- (16) Ott Weist, A.; Glandt, E. D. *J. Chem. Phys.* **1994**, *101*, 5167.
- (17) Perram, J. W.; Smith, E. R. *Proc. R. Soc. London, Ser. A.* **1977**, *353*, 193. Kierlik, E.; Rosinberg, M. L. *Mol. Phys.* **1989**, *68*, 867. Holovko, M. F.; Vakarin, E. V.; Duda, Yu. Ya. *Chem. Phys. Lett.* **1995**, *233*, 420.
- (18) Badiali, J. P.; Blum, L.; Rosinberg, M. L. *Chem. Phys. Lett.* **1986**, *129*, 149. Blum, L. *Adv. Chem. Phys.* **1990**, *78*, 171. Holovko, M. F.; Vakarin, E. V. *Chem. Phys. Lett.* **1994**, *230*, 507. Vakarin, E. V.; Holovko, M. F. *Mol. Phys.* **1997**, *90*, 63.
- (19) Henderson, D.; Abraham, F. F.; Barker, J. A. *Mol. Phys.* **1976**, *31*, 1291. Holovko, E. V.; Vakarin, E. V. *Mol. Phys.* **1995**, *84*, 1057; **1996**, *87*, 123.
- (20) Holovko, E. V.; Vakarin, E. V. *Mol. Phys.* **1996**, *87*, 1375.
- (21) Ghonasgi, D.; Chapman, W. G. *J. Chem. Phys.* **1995**, *102*, 2585.
- (22) Beizer, M. M.; Lund, H. *Organic electrochemistry. Introduction and Guided*; Dekker: New York, 1983.
- (23) Minko, S. S.; Luzinov, I. A.; Voronov, A. S. *Colloid J.* **1994**, *56*, 720.
- (24) Cassie, A. B. D.; Baxter, S. *Trans. Faraday Soc.* **1944**, *40*, 546.
- (25) Rayss, J.; Widomski, J.; Luzinov, I. A.; Voronov, A. S.; Minko, S. S. *J. Appl. Polym. Sci.*, to be published.
- (26) Pefferkorn, E. *Adv. Colloid Interface Sci.* **1995**, *56*, 33.

MA970444O